A polyisoindigo derivative as novel n-type conductive binder inside Si@C nanoparticle electrodes for Li-ion battery applications

Adrien Mery, Pierre Bernard, Anthony Valero, John Alper, Nathalie Herlin-Boime, Cédric Haon, Florence Duclairoir, Said Sadki

A polyisoindigo derivative as novel n-type conductive binder inside Si@C nanoparticle electrodes for Li-ion battery applications

Adrien Mery[1], Pierre Bernard[2], Anthony Valero[1], John P. Alper[3], Nathalie Herlin-Boime[3], Cédric Haon[2], Florence Duclairoir[1], Said Sadki[1]

[1] Univ. Grenoble Alpes, CEA, CNRS, INAC-SyMMES, F-38000 Grenoble, France.

[2] Univ. Grenoble Alpes, CEA, LITEN, F-38054 Grenoble, France

[3] Université Paris Saclay, IRAMIS, UMR NIMBE, CEA Saclay, F91191 Gif-sur-Yvette, France

Corresponding Author

*Saïd Sadki, Corresponding author email: said.sadki@cea.fr

Abstract

Herein we report the successful use of a polyisoindigo derivative (P(iso)) as a new conductive binder inside electrode formulations containing silicon nanoparticles covered with a carbon shell (Si@C) for Li-ion batteries. The expected role of the carbon shell is to stabilize the Solid Electrolyte Interphase layer (SEI) to prevent it from cracking under nanoparticle volume variations during lithiation processes. The P(iso) conducting polymer is used to act both as mechanical binder and n-type conductive component in replacement of usual carbonaceous additive materials. Ultimately, the cumulative contributions of both materials inside a two-electrode component formulation (Si@C-P(iso)) aim to address the stability drawbacks commonly faced by silicon electrodes. Physico-chemical characterizations revealed that the Si@C nanoparticles are uniformly embedded inside the polymeric matrix. Electrochemical measurements in half-cells clearly show the formation of Li-Si alloys during cycling. Moreover specific capacities up to 1400 mAh/g with a remarkable stability until 500 cycles have been achieved, proving this conductive polymer to be a valid alternative to classical polymeric binders mixed with carbonaceous additives. These very promising results highlight the use

of this polyisoindigo family as new conductive binders inside Si@C electrode formulations for Li-ion battery applications.

Keywords

Si@C nanoparticles; Li-ion battery; n-type conductive polymer binder; electrode formulation; polyisoindigo

1. Introduction

Nowadays, electrochemical devices for energy storage have become essential for several applications such as portable electronic devices and electrical vehicles [1,2]. Particularly Li-ion batteries have met market since the early 1990's, mainly in the portable domain. However, commercial batteries do not yet meet requirements for high energy applications partly due to the limitation imposed by the negative graphite electrode (theoretical capacity of 372 mAh/g). Thus, batteries with higher energy densities and enhanced cycle life is still a great challenge for electrical vehicles. [3–7].

One efficient way to increase the energy density of Li-ion batteries is the elaboration of electrode materials with higher specific and volumetric capacities. During the past few years, the use of silicon as active material has been greatly studied by the energy storage community. Indeed, Li_xSi_y is an alloy-type material of choice among the negative electrode candidates due to the relatively high theoretical specific capacity of silicon (3579 mAh/g), its scale up availability and low-cost [8–11]. Unfortunately, several drawbacks arise for silicon based materials and must be overcome to turn into a viable solution as stable negative electrode. Indeed, all along cycling, phase transformations suffered by silicon during the alloy formation with lithium lead to drastic volume changes of the material (> 300%). Also, due to the low potential of silicon electrodes (0.01V to 1V vs Li^+/Li) solvents from electrolytes decompose to form a SEI (Solid-Electrolyte Interphase) on electrode surfaces [12]. The overall mechanical stress leads to fracture and pulverization of silicon together with the partial destruction and reconstruction of the SEI (Solid-Electrolyte Interphase) preventing an effective and permanent passivation of the electrode. Ultimately, the association of pulverized material and

continuous formation of non-stable SEI results in a global volume increasing of the electrode and in the delamination of silicon material from the current collector leading to a degradation of the Li-ion cell [10,13,14].

Several strategies are followed to tackle these drawbacks such as the nanostructuration of silicon particles to limit the pulverization or the synthesis of silicon composites wrapped by carbon materials (Si@C) to buffer volume changes and stabilize SEI [8,15,16]. Different methods are used to synthesize these composite materials like CVD, sol-gel synthesis, laser pyrolysis or the elaboration of complex structures as "Yolk-Shell" type [17–19].

Currently, studies are increasingly moving from the elaboration of the Si active material toward the optimization of the overall electrode formulation [20]. Particularly, research on new binder materials which are necessary for the structural and mechanical stability of the Si-based electrode is an emerging field [21]. Many insulating polymeric binders such as carboxymethyl cellulose (CMC), polyvinylidene fluoride (PVDF), polytetrafluoroethylene (PTFE), polyacrylic acid (PAA) are used in electrode formulations with the addition of conductive carbonaceous materials [22,23]. More recently, studies have shifted toward the use of conducting polymers as binders in replacement of these classical insulating binders. Their expected role is to work as both binder and conductive agent avoiding the use of carbonaceous conductive additives. Moreover, the simplified electrode formulation may contain more active material, leading to potential higher gravimetric and volumetric capacities per total mass of the electrode [20,24,25]. Up to now, few works have been conducted onto this association of conducting polymer with Si or Si@C nanoparticles but it remains an emerging and challenging field [20,24–26].

In this context, the scope of this work consist on the elaboration of a new electrode formulation containing Si@C nanoparticles mixed with a conductive polymer binder to promote SEI and conductive network preservation. The elaborated and tested conjugated polymer belongs to the polyisoindigo family. Reynold's group and others, have been working for several years on these conductive polymers for organic field effect transistors (OFETs) and organic photovoltaics (OPVs)

applications. They demonstrated their n-type behavior and their ability to work at low potentials [27–29]. We strongly believe that the properties of conduction, the mechanical and electrochemical stabilities of these polymers are also attractive for battery electrode formulations. Thus, the motivation of this study was to investigate the polyisoindigo as new n- type conductive binders for Si@C electrode and thereby broadening their field of applications. Also, the objective was to improve the stability of the Si@C electrode and suppress the carbon additives inside the electrode formulation. Physico-chemical characterizations were conducted on the Si@C-P(iso) materials to evidence Si@C nanoparticles embedment inside polymer matrix and tests in half-cells were performed to evaluate their electrochemical performances. To the best of our knowledge it is the first application of the polyisoindigo family as conductive binder inside silicon/Si@C electrodes and more generally in the Li-ion battery domain.

2. Results and discussion

Si@C nanoparticles have been chosen because the C shell can reduce SEI instability due to the stress experienced by silicon cores during cycling and also favor the interaction with the polymer. They were synthesized by laser pyrolysis which has already been described in a previous work [19] and more details are available in Supporting Information (**Experimental section**). P(iso) synthesis was elaborated by using Yamamoto cross-coupling reaction with the $Ni(COD)_2$ catalyst in place of Suzuki coupling traditionally used by other groups [27,28]. This choice was made because this organometallic cross-coupling reaction leads to the synthesis of the polymer in a single step while Suzuki coupling requires intermediate steps involving the formation of a diborylated monomer. P(iso) was chosen because of its aromaticity. Preferential interactions are likely to arise between the C shell from the Si@C nanoparticles and the conjugated backbone of the polymer, stabilizing the nanoparticles surface but also preserving electrical contact between active material and binder. It is interesting to note that when Piso and Si nanoparticles not bearing a C shell are mixed, the slurry obtained is non homogeneous and leads to cracked electrodes avoiding concluding and reproducible electrochemical measurements. This macroscopic observation show that uncracked electrodes

may only be obtained when preferential interactions can occur between C shell and polymeric matrix. The good electrochemical stability demonstrated by Reynold's et al. have motivated also our choice as the final formulation should be able to cycle over time. The obtained polymer is then mixed as conductive binder with Si@C nanoparticles and the resulting mixture is coated on a copper foil used as current collector to obtain electrodes which are inserted inside electrochemical half-cells (**Fig. 1**). All the synthesis steps and electrode preparation processes are described in Supporting Information (**Experimental section**).

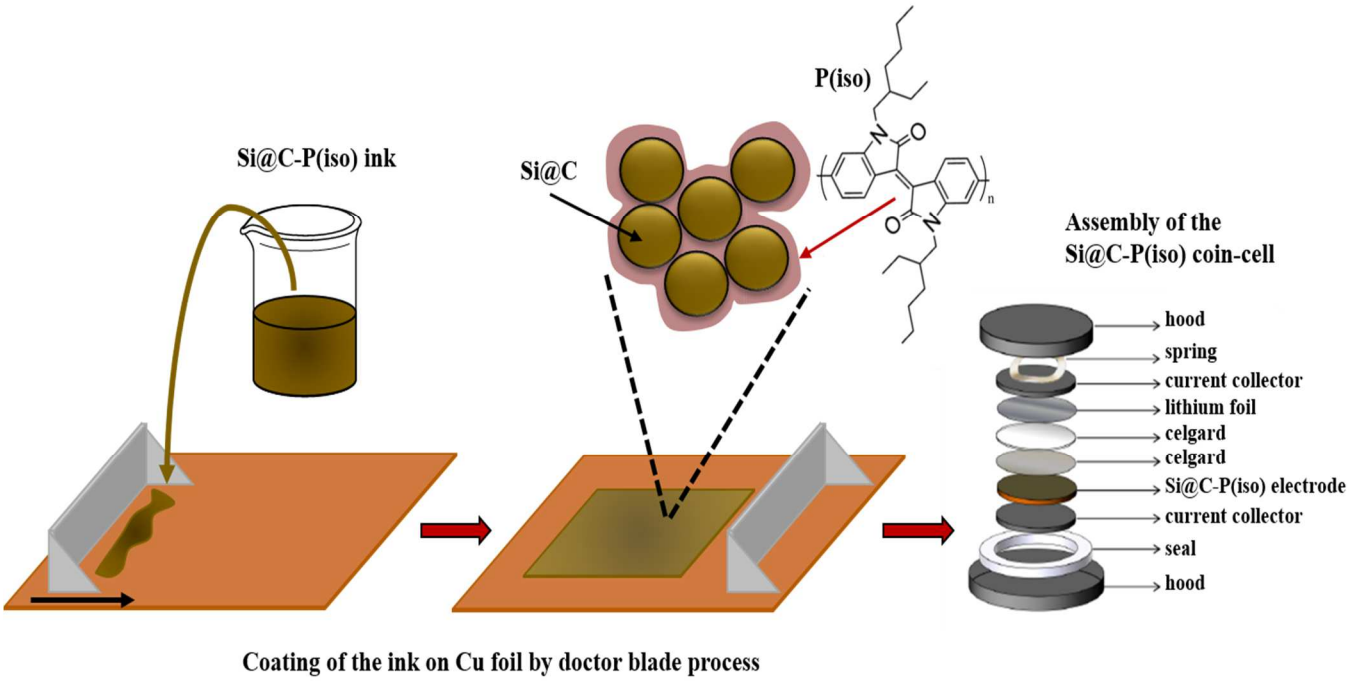

Fig. 1. Scheme of electrode formulation and half-cell assembly.

The structural and chemical characterizations of the electrode materials are presented in **Fig. 2**. SEM images of Si@C-P(iso) electrodes at different magnifications (**Fig. 2a and 2b**) give a glimpse of the interaction between the polymer and the Si@C nanoparticles. Si@C nanoparticles embedded inside a polymer matrix can be observed mainly at high magnification (**Fig. 2b**). These images reveal that a polymeric network seems to connect small aggregates of Si@C nanoparticles together. These

morphological observations highlight the polyisoindigo ability to mix homogeneously with and interconnect Si@C nanoparticles, as expected for a binder.

TEM images (**Fig. S3 a and b**) bring additional information concerning the size of the Si@C nanoparticles. The diameter range observed is between 20 nm and 40 nm. Moreover the magnified TEM images clearly highlight the crystallinity of the nanoparticles core as crystalline planes can be observed. This crystalline structure is also confirmed by the XRD diffractogram of Si@C nanoparticles in supporting information (**Fig. S4**). To clearly evidence the carbon shell around the silicon particles, we performed a STEM-EELS observation of the Si@C nanoparticles without P(iso) (**Fig. S3c)**. This STEM-EELS image clearly highlights the presence of the carbon shell (in red) around the Si nanoparticles (in green)

Survey XPS spectra have been recorded on both Si@C nanoparticles and Si@C-P(iso) formulation (**Fig. 2c**) to clearly confirm the presence of the conductive polymer well mixed with Si@C nanoparticles inside the formulation. Both spectra show the presence of C1s (284 eV), O1s (530 eV) and Si2p (99 eV) elements, however the spectra of the Si@C-P(iso) formulation displays additional signals of N1s (399 eV) and Br3d (70 eV) that are clear signatures of the presence of the polymer. Indeed the N elements come from the pyrrolidine groups from the isoindigo unit and the Br – being the active halide in the coupling reaction - are expected to be present on the terminal positions of the polymer. For the Si@C-P(iso) formulation, the Si2p signal is still clearly visible, hence it can be stated that the polymer layer remains thin (<5 nm).

C1s core-level high resolution spectra for the Si@C-P(iso) formulation (**Fig. 2d**) and the bare Si@C (**Fig. 2e)** have been recorded and deconvoluted. The C1s signal of the bare Si@C arises from the C shell and has been deconvoluted into different components. A signal attributed to C of silicon carbide can be seen at 282.8 eV, as well as a signal from sp^2 Cs at 284.3 eV. Other C peaks observed at 286.1 eV, 288.1 eV and 289.6 eV can be attributed to oxygen containing functions (C-O, C=O, COO respectively) indicating that the C shell is a defective conjugated network [30]. The C shell of the Si@C nanoparticles being stable under the mixing conditions at RT with the polymeric binder, these

C1s spectral components have been fixed and used to deconvolute the C1s signal obtained for the Si@C-P(iso) formulation. Consequently, the complementary contributions at 284.2 eV, 285.5 eV and 287.6 eV can be respectively attributed to C assigned to sp^2, C-N bond and C=O of the polymer (**Fig. 2d**). The HR N1s spectra confirms the presence of N coming from the polymer (**Fig. 2f**). The C(N)/N atomic concentration ratio of 3:1 corresponds to the pyrrolidinic unit of the polymer (**Table S1**). These characterizations argue that Si@C and P(iso) seem intimately linked together inside the electrode formulation.

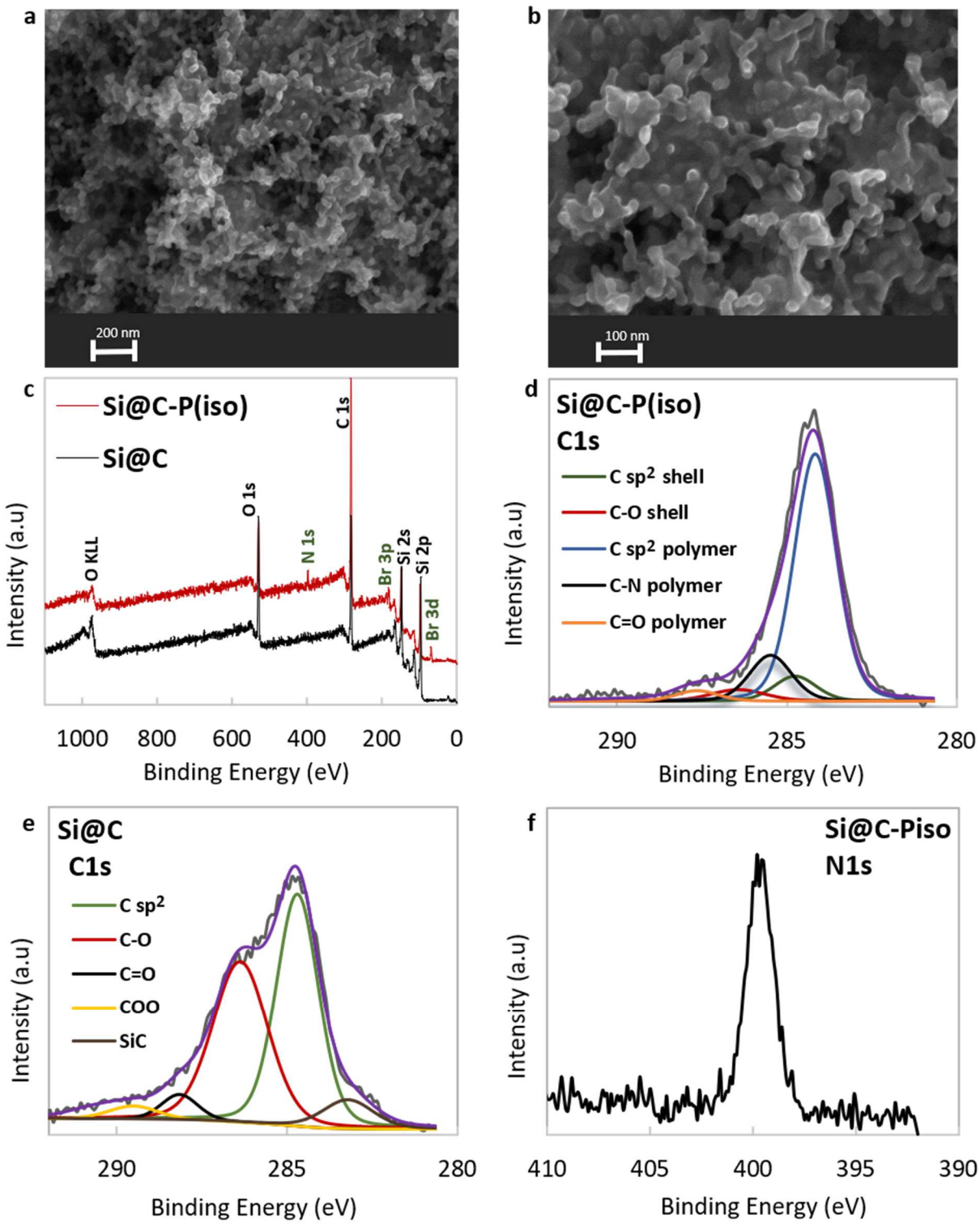

Fig. 2. Structural and chemical characterizations of the Si@C-P(iso) material. SEM image (a) and SEM image magnified (b), XPS survey spectra of both Si@C and Si@C-P(iso) (c) and XPS C1s HR spectra deconvolution for Si@C-P(iso) (d) and bare Si@C nanoparticles (e) and XPS N1s HS spectrum of Si@C-Piso material (f)

Battery tests were performed in half-cells consisting of Si@C-P(iso) formulation (75% / 25% mass ratio) as working electrode versus a lithium foil as counter electrode. The electrolyte solution is 1M $LiPF_6$ in EC: DEC (1:1) with 10% FEC and 2% VC. All charge/discharge rates were calculated by considering the total mass of the electrode and the theoretical capacity of the silicon material (3579 mAh/g). Gravimetric specific capacity values are calculated with respect to the mass of Si active material (between 0.4 and 0.6 mg).

Fig. 3a displays the cyclic voltammogramm of Si@C-P(iso) half-cell at different cycles at a scan rate of 20µV/s. The expected behavior of lithiation/delithiation processes showing the Li-Si alloy formations is clearly displayed and in agreement to that observed with common Si(or Si@C) electrode formulations [19,31]. In our study, a gradual increase of the current is observed during the 10-15 first cycles and is assigned to a deep and more effective lithiation of the material. After the 15^{th} cycle, a steady signal is reached and suggests a complete and reversible lithiation/delithiation process during cycling. Such behavior makes this P(iso) conductive binder a suitable alternative to common insulating polymeric binders used with carbonaceous additives inside Si@C electrode formulations.

First lithiation/delithiation galvanostatic curve is shown on **Fig. 3b** (black curve). A low charge/discharge rate of C/20 is applied during this first cycle to allow a complete and deep lithiation of the Si@C nanoparticles. The capacity achieved during this first lithiation process is 3507 mAh/g which is close to the theoretical capacity expected for silicon material. However, an important amount of the lithium ions mainly consumed for the SEI formation is not recovered during the first delithiation process. An irreversible capacity around 49% appears after the first charge/discharge cycle (corresponding to a recovered capacity of 1800 mAh/g), which is high but not so far from irreversible capacities reported in the literature for Si-based electrodes (around 30-40%). In Si@C-P(iso) electrode, the formulation consists only of Si@C nanoparticles mixed with P(iso) conductive polymer binder without other additives which is different from a conventional three components electrode where carbonaceous additives are added for the conductivity of the electrode. Interfaces between

electrode and electrolyte might be different in our two component formulation, leading certainly to a different nature of the SEI and to a larger consumption of Li^+ during the irreversible process.

Cycling tests were then performed on Si@C-P(iso) half-cells at a C rate of C/5. Galvanostatic curves for the 20^{th}, 50^{th}, 100^{th}, 200^{th} and 300^{th} cycles are also presented in **Fig. 3b**. It is worth noting that the capacity increases between the 20^{th} and the 100^{th} cycle, then stabilizes until the 300^{th} cycle, highlighting the good stability of the electrochemical system and the non-damaging consequence of the first irreversible capacity on the stability.

This trend is clearly shown in **Fig. 3c** representing the specific capacity as a function of cycle numbers and the efficiency of the half-cell. The shape of the capacity curve during cycling is particularly distinctive (**Fig. 3c** black curve) as three domains can be observed: an important decrease of the capacity during the first 20 cycles followed by a constant increase over approximately the next 80 cycles and finally a stabilization of the capacity around 1450-1480 mAh/g until the 300^{th} cycle. This behavior can be explained by the swelling and an internal structural reorganization of the polymer occurring in the two first domains. Indeed, it is well known from the literature that a change in reduction state of the polymer results in the diffusion of solvated ions between the polymer and the surrounding electrolyte to maintain charge neutrality [32]. The solvated ion transport in and out of the polymer matrix is generally thought to be the main cause of the expansion and contraction of the polymers. Small ions like solvated Li^+ can leave and enter the polymer during the n-doping/de-doping phenomena occurring in P(iso) binder. This controlled diffusion is kinetically slow and the polymer matrix inside the electrode reach a thermodynamic equilibrium after 100 cycles with high gravimetric capacities and excellent retention.

A magnification of the coulombic efficiency is showed in **Fig. 3c (inset)**. An average efficiency of 99.56% is reached after 300 cycles. Moreover, a high efficiency between 99.7 and 100% is achieved over the last 100 cycles, after the capacity stabilization of the device, which demonstrate very encouraging efficiency results. Once stabilized, P(iso) binder interacting strongly with the Si@C nanoparticles, brings the expected robustness and conductivity to the electrochemical system.

To further evidence the beneficial contribution of the P(iso) as conductive binder, a comparison between the electrochemical performances of Si@C-P(iso) electrode formulation and more conventional Si@C/CMC/CB formulation was performed (**Fig. 3d.**). It clearly appears that the capacity retention and the stability are greatly improved within the Si@C-P(iso) electrode. Indeed, after 250 cycles, the Si@C-P(iso) half-cell maintain its maximal capacity while the capacity of the Si@C/CMC/CB half-cell drops continually and only 55% of the initial capacity is recovered after 250 cycles. These results clearly highlight the good resilience and performances of the Si@C-P(iso) electrode formulation and validate the increased electrochemical performances of this electrode formulation without carbon black additive.

Finally, power tests were also carried out on Si@C-P(iso) half-cell and the results are displayed in **Fig. 3e**. An obvious decrease of the capacity is observed when increasing the charge/discharge rate (from C/5 to 2C), as expected when ion transport kinetics increase, and the capacity clearly drops at 2C. However, the high stability of the system evidenced at C/5 until 500 cycles is unequivocally a very interesting result. Indeed, even after cycling at 2C, a similar behavior to that obtained for the initial C/5 cycling (**Fig. 3c.**) is observed. Although capacities decrease at higher charging/discharging rates, the performances are recovered and stable when the system returns to C/5. Thus, there is no harmful effect experienced by the electrochemical system when increasing the C rate, indicating the high stability of the P(iso) binder and the overall electrode formulation. These results highlight the high performances and durability of the Li-ion device and the expected contribution of the polyisoindigo derivative as conductive binder inside the Si@C electrode formulations.

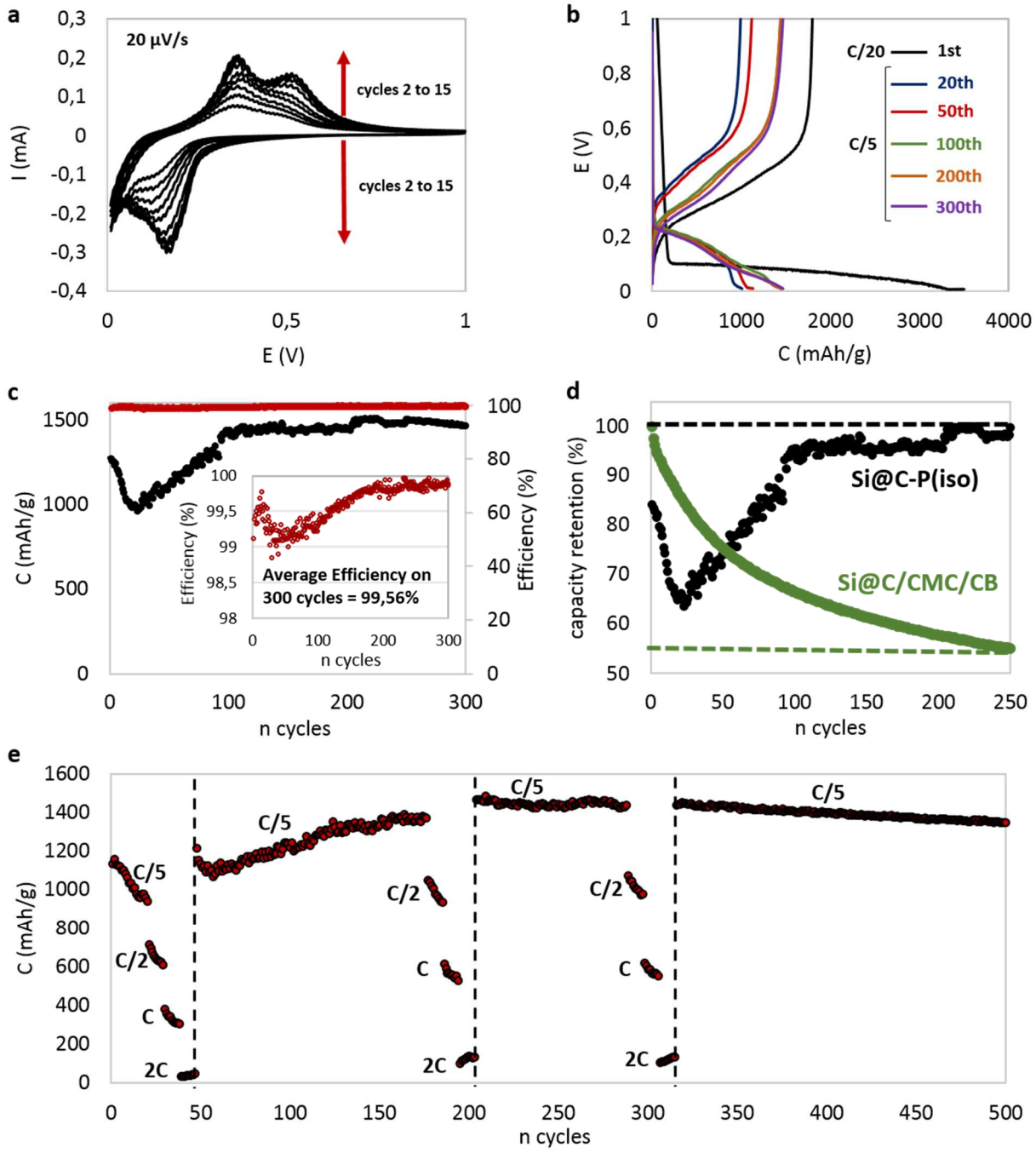

Fig. 3. Battery performances of the Si@C-P(iso) half-cells in 1M $LiPF_6$ in EC: DEC (1:1) with 10% FEC and 2% VC battery electrolyte. Cyclic voltammogramm at 20 µV/s (a), galvanostatic profiles at different cycles (b), stability of the capacity at C/5 as a function of the cycle numbers and magnification of the coulombic efficiency of the device in the inset (c), comparison of the capacity retention of the Si@C-P(iso) electrode (black curve) and the Si@C/CMC/CB electrode (green curve) at C/5 (d) and power tests of the Si@C-P(iso) half-cell at different charge/discharge rates (e).

3. Conclusions

In this study a polyisoindigo derivative was successfully elaborated by Yamamoto cross-coupling reaction and tested as new conductive binder for Si@C electrode formulations. SEM images cumulated with XPS analyses clearly show the presence of the polyisoindigo derivative inside the Si@C electrode formulations. Electrochemical results in half-cells highlight the high stability of the Si@C-P(iso) electrode formulation over 500 cycles with capacities that remains as high as 1400 mAh/g. Moreover, electrochemical stability during cycling is improved compared to a traditional Si@C/CMC/CB half-cell. Thus, the successful use of the electrode formulation containing only two components, Si@C nanoparticles as active material and the conducting polymer playing the role of both binder and conductive additive, has been demonstrated. Moreover, the potential use of a polyisoindigo conducting polymer as a novel conductive binder inside Si@C electrode formulations has been established. It is to the best of our knowledge the first time that this polymer family has been used as conductive binder inside silicon electrode formulations and more generally in Li-ion battery applications. This work paves the way to the testing of a whole class of n-type conductive polymers, up to now mainly dedicated to OFETs and OPVs, for battery applications.

Acknowledgments

This work has been performed in the SIBALI project in the framework of the CEA program “Plan de couplage DRF-DRT”

The authors want to thank Dr. Anass Benayad for XPS measurements. They want to thank B.S. student Juliette Tiberghien and PhD student Gauthier Menassol for preliminary works on isoindigo derivatives. We also want to thank PhD student Olivier Bardagot, Dr. Cyril Aumaitre and Yann Kervella for their advices concerning polymer synthesis. Finally authors are grateful to Aurélie Habert for XRD measurements and carbon content evaluation in Si@C nanoparticles.

Appendix A. Supporting information

References

[1] M.A. Hannan, M.M. Hoque, A. Mohamed, A. Ayob, Review of energy storage systems for electric vehicle applications: Issues and challenges, Renew. Sustain. Energy Rev. 69 (2017) 771–789. doi:10.1016/j.rser.2016.11.171.

[2] B. Dunn, H. Kamath, J.-M. Tarascon, Electrical Energy Storage for the Grid: A Battery of Choices, Science. 334 (2011) 928–935. doi:10.1126/science.1212741.

[3] C.K. Chan, H. Peng, G. Liu, K. McIlwrath, X.F. Zhang, R.A. Huggins, Y. Cui, High-performance lithium battery anodes using silicon nanowires, Nat. Nanotechnol. 3 (2008) 31–35.

[4] J.-Y. Li, Q. Xu, G. Li, Y.-X. Yin, L.-J. Wan, Y.-G. Guo, Research progress regarding Si-based anode materials towards practical application in high energy density Li-ion batteries, Mater. Chem. Front. (2017). doi:10.1039/C6QM00302H.

[5] G.E. Blomgren, The Development and Future of Lithium Ion Batteries, J. Electrochem. Soc. 164 (2017) A5019–A5025.

[6] L. Wang, G. Zhang, Q. Liu, H. Duan, Recent progress in Zn-based anodes for advanced lithium ion batteries, Mater. Chem. Front. 2 (2018) 1414–1435. doi:10.1039/C8QM00125A.

[7] J. Liu, X. Xu, R. Hu, L. Yang, M. Zhu, Uniform Hierarchical Fe3O4@Polypyrrole Nanocages for Superior Lithium Ion Battery Anodes, Adv. Energy Mater. 6 (2016) 1600256. doi:10.1002/aenm.201600256.

[8] W.-J. Zhang, A review of the electrochemical performance of alloy anodes for lithium-ion batteries, J. Power Sources. 196 (2011) 13–24. doi:10.1016/j.jpowsour.2010.07.020.

[9] M.T. McDowell, S.W. Lee, W.D. Nix, Y. Cui, 25th Anniversary Article: Understanding the Lithiation of Silicon and Other Alloying Anodes for Lithium-Ion Batteries, Adv. Mater. 25 (2013) 4966–4985. doi:10.1002/adma.201301795.

[10] X. Zuo, J. Zhu, P. Müller-Buschbaum, Y.-J. Cheng, Silicon based lithium-ion battery anodes: A chronicle perspective review, Nano Energy. 31 (2017) 113–143.

[11] K. Feng, M. Li, W. Liu, A.G. Kashkooli, X. Xiao, M. Cai, Z. Chen, Silicon-Based Anodes for Lithium-Ion Batteries: From Fundamentals to Practical Applications, Small. (n.d.) n/a-n/a. doi:10.1002/smll.201702737.

[12] T. Yoon, M.S. Milien, B.S. Parimalam, B.L. Lucht, Thermal Decomposition of the Solid Electrolyte Interphase (SEI) on Silicon Electrodes for Lithium Ion Batteries, Chem. Mater. 29 (2017) 3237–3245. doi:10.1021/acs.chemmater.7b00454.

[13] K. Rhodes, N. Dudney, E. Lara-Curzio, C. Daniel, Understanding the Degradation of Silicon Electrodes for Lithium-Ion Batteries Using Acoustic Emission, J. Electrochem. Soc. 157 (2010) A1354–A1360. doi:10.1149/1.3489374.

[14] X.H. Liu, L. Zhong, S. Huang, S.X. Mao, T. Zhu, J.Y. Huang, Size-Dependent Fracture of Silicon Nanoparticles During Lithiation, ACS Nano. 6 (2012) 1522–1531. doi:10.1021/nn204476h.

[15] J. R. Szczech, S. Jin, Nanostructured silicon for high capacity lithium battery anodes, Energy Environ. Sci. 4 (2011) 56–72. doi:10.1039/C0EE00281J.

[16] N. Liu, Z. Lu, J. Zhao, M.T. McDowell, H.-W. Lee, W. Zhao, Y. Cui, A pomegranate-inspired nanoscale design for large-volume-change lithium battery anodes, Nat. Nanotechnol. 9 (2014) 187–192. doi:10.1038/nnano.2014.6.

[17] U. Kasavajjula, C. Wang, A.J. Appleby, Nano- and bulk-silicon-based insertion anodes for lithium-ion secondary cells, J. Power Sources. 163 (2007) 1003–1039. doi:10.1016/j.jpowsour.2006.09.084.

[18] N. Liu, H. Wu, M.T. McDowell, Y. Yao, C. Wang, Y. Cui, A Yolk-Shell Design for Stabilized and Scalable Li-Ion Battery Alloy Anodes, Nano Lett. 12 (2012) 3315–3321. doi:10.1021/nl3014814.

[19] J. Sourice, A. Quinsac, Y. Leconte, O. Sublemontier, W. Porcher, C. Haon, A. Bordes, E. De Vito, A. Boulineau, S. Jouanneau Si Larbi, N. Herlin-Boime, C. Reynaud, One-Step Synthesis of Si@C Nanoparticles by Laser Pyrolysis: High-Capacity Anode Material for Lithium-Ion Batteries, ACS Appl. Mater. Interfaces. 7 (2015) 6637–6644. doi:10.1021/am5089742.

[20] T.M. Higgins, S.-H. Park, P.J. King, C. Zhang, N. McEvoy, N.C. Berner, D. Daly, A. Shmeliov, U. Khan, G. Duesberg, A Commercial Conducting Polymer as Both Binder and Conductive Additive for Silicon Nanoparticle-Based Lithium-Ion Battery Negative Electrodes, ACS Nano. 10 (2016) 3702–3713.
[21] P.-F. Cao, M. Naguib, Z. Du, E. Stacy, B. Li, T. Hong, K. Xing, D.N. Voylov, J. Li, D.L. Wood, A.P. Sokolov, J. Nanda, T. Saito, Effect of Binder Architecture on the Performance of Silicon/Graphite Composite Anodes for Lithium Ion Batteries, ACS Appl. Mater. Interfaces. 10 (2018) 3470–3478. doi:10.1021/acsami.7b13205.
[22] Song Jiangxuan, Zhou Mingjiong, Yi Ran, Xu Terrence, Gordin Mikhail L., Tang Duihai, Yu Zhaoxin, Regula Michael, Wang Donghai, Interpenetrated Gel Polymer Binder for High-Performance Silicon Anodes in Lithium-ion Batteries, Adv. Funct. Mater. 24 (2014) 5904–5910. doi:10.1002/adfm.201401269.
[23] L. Chen, X. Xie, J. Xie, K. Wang, J. Yang, Binder effect on cycling performance of silicon/carbon composite anodes for lithium ion batteries, J. Appl. Electrochem. 36 (2006) 1099–1104. doi:10.1007/s10800-006-9191-2.
[24] S. Huang, J. Ren, R. Liu, M. Yue, Y. Huang, G. Yuan, The progress of novel binder as a non-ignorable part to improve the performance of Si-based anodes for Li-ion batteries, Int. J. Energy Res. (n.d.) n/a-n/a. doi:10.1002/er.3826.
[25] G. Liu, S. Xun, N. Vukmirovic, X. Song, P. Olalde-Velasco, H. Zheng, V.S. Battaglia, L. Wang, W. Yang, Polymers with tailored electronic structure for high capacity lithium battery electrodes, Adv. Mater. 23 (2011) 4679–4683.
[26] D. Liu, Y. Zhao, R. Tan, L.-L. Tian, Y. Liu, H. Chen, F. Pan, Novel conductive binder for high-performance silicon anodes in lithium ion batteries, Nano Energy. 36 (2017) 206–212. doi:10.1016/j.nanoen.2017.04.043.
[27] R. Stalder, J. Mei, K.R. Graham, L.A. Estrada, J.R. Reynolds, Isoindigo, a Versatile Electron-Deficient Unit For High-Performance Organic Electronics, Chem. Mater. 26 (2014) 664–678. doi:10.1021/cm402219v.
[28] R. Stalder, J. Mei, J. Subbiah, C. Grand, L.A. Estrada, F. So, J.R. Reynolds, n-Type conjugated polyisoindigos, Macromolecules. 44 (2011) 6303–6310. http://pubs.acs.org/doi/abs/10.1021/ma2012706 (accessed March 23, 2017).
[29] F. Grenier, P. Berrouard, J.-R. Pouliot, H.-R. Tseng, A. J. Heeger, M. Leclerc, Synthesis of new n-type isoindigo copolymers, Polym. Chem. 4 (2013) 1836–1841. doi:10.1039/C2PY20986A.
[30] S. Stankovich, D.A. Dikin, R.D. Piner, K.A. Kohlhaas, A. Kleinhammes, Y. Jia, Y. Wu, S.T. Nguyen, R.S. Ruoff, Synthesis of graphene-based nanosheets via chemical reduction of exfoliated graphite oxide, Carbon. 45 (2007) 1558–1565. doi:10.1016/j.carbon.2007.02.034.
[31] J. Lin, J. He, Y. Chen, Q. Li, B. Yu, C. Xu, W. Zhang, Pomegranate-Like Silicon/Nitrogen-doped Graphene Microspheres as Superior-Capacity Anode for Lithium-Ion Batteries, Electrochimica Acta. 215 (2016) 667–673. doi:10.1016/j.electacta.2016.08.147.
[32] C. Bohn, S. Sadki, A.B. Brennan, J.R. Reynolds, In Situ Electrochemical Strain Gage Monitoring of Actuation in Conducting Polymers, J. Electrochem. Soc. 149 (2002) E281–E285. doi:10.1149/1.1486451.